State of Radiomics in Glioblastoma

Birra Taha, MD*
Daniel Boley, PhD‡
Ju Sun, PhD‡
Clark C. Chen, MD, PhD*

*Department of Neurosurgery, University of Minnesota, Minneapolis, Minnesota, USA; ‡Department of Computer Science and Engineering, University of Minnesota, Minneapolis, Minnesota, USA

Correspondence:
Clark C. Chen, MD, PhD,
University of Minnesota Neurosurgery,
D429 Mayo Memorial Building,
420 Delaware St SE, MMC96,
Minneapolis, MN 55455, USA.
Email: ccchen@umn.edu

Received, August 1, 2020.
Accepted, February 13, 2021.

Radiomics is an emerging discipline that aims to make intelligent predictions and derive medical insights based on quantitative features extracted from medical images as a means to improve clinical diagnosis or outcome. Pertaining to glioblastoma, radiomics has provided powerful, noninvasive tools for gaining insights into pathogenesis and therapeutic responses. Radiomic studies have yielded meaningful biological understandings of imaging features that are often taken for granted in clinical medicine, including contrast enhancement on glioblastoma magnetic resonance imaging, the distance of a tumor from the subventricular zone, and the extent of mass effect. They have also laid the groundwork for noninvasive detection of mutations and epigenetic events that influence clinical outcomes such as isocitrate dehydrogenase (IDH) and O^6-methylguanine-DNA methyltransferase (MGMT). In this article, we review advances in the field of glioblastoma radiomics as they pertain to prediction of IDH mutation status and MGMT promoter methylation status, as well as the development of novel, higher order radiomic parameters.

KEY WORDS: Radiomics, Glioblastoma, Radiogenomics, Imaging, Neuro-oncology

Neurosurgery 0:1–8, 2021 DOI:10.1093/neuros/nyab124 www.neurosurgery-online.com

The fundamental premise of modern oncology is built on tailoring therapy to cancer vulnerabilities unveiled by analysis of the surgically acquired specimens.[1] While surgical excision or biopsy is generally safe, the risk associated with the procedure can be significant, particularly in brain cancer.[2] The surgical risk is further magnified in situations where serial biopsies are required due to regional heterogeneity.[3] Even in surgeries performed without complications, patients are left with discomfort and surgery-associated stress.[4,5] Moreover, challenges related to spatial sampling errors,[6] intratumoral heterogeneity,[7,8] and timeliness of biopsy[6,9] pose formidable obstacles in surgical planning.

ABBREVIATIONS: 2HG, 2 hydroxyglutarate; **ADC,** apparent diffusion coefficient; **CE,** contrast enhancement; **DKI,** diffusion kurtosis imaging; **DSC,** dynamic susceptibility contrast; **IDH,** isocitrate dehydrogenase; **LVd,** lateral ventricle displacement; **MGMTp,** MGMT promoter; **MNI,** Montreal Neurological Institute; **PRC,** precision-recall curve; **rCBV,** relative cerebral blood volume; **SVZ,** subventricular zone; **SVZd,** distance to the subventricular zone; **TCIA,** The Cancer Imaging Atlas; **VEGF,** vascular endothelial growth factor

Magnetic resonance imaging (MRI) has traditionally played roles limited to diagnostic and postsurgical evaluation. rising field of radiomics has began to expand these roles.[10,11] Radiomics refers to the systematic extraction and analysis of features derived from medical images. Pertaining to neuro-oncology, the association between quantitative features and clinical outcome and tumor physiology offers the promise of a radiomic biopsy (dubbed a "radiopsy"[12]), with potential for evidence-based clinical decision making without surgery. Moreover, radiomics leverages the spatial breadth of imaging to capture information about regions beyond the tumor borders and into the peritumoral space, where surgical biopsies are not routinely performed.[13] Synthesis of radiomics with novel physiological imaging platforms may offer insights into molecular physiology invisible to the standard analysis of surgical biopsy specimens.[14]

In this context, there is mounting interest in the clinical application of radiomics to virtually every aspect of neuro-oncology that involves imaging, with exponential growth in the volume of peer-reviewed publications.[15] From survival prognostication[16] to diagnostic determination to mutational profiling, the voluminous literature prohibits an exhaustive

review here. Instead, we focus our review on the prognostic utility of radiomics in glioblastomas, the most common form of primary brain cancer in adults.[17] In particular, we examined radiomics as it pertains to the prediction of isocitrate dehydrogenase (IDH) mutation status and O^6-methylguanine-DNA methyltransferase (MGMT) promoter methylation status. We further discuss the development of higher order, survival-associated radiomic features, including contrast enhancement (CE), distance of a glioblastoma from the subventricular zone (SVZd), and glioblastoma-associated mass effect. We define all relevant abbreviations used in this manuscript in Table.

GENERAL OVERVIEW OF RADIOMICS

Radiomics is a multistep process that can be applied to any set medical images, including a spectrum of MRI modalities involving both conventional (T1, T2, etc) and more advanced imaging (diffusion tensor imaging, susceptibility-weighted imaging, etc).[18-20] These steps include image processing, image segmentation, feature extraction, model building, and validation (Figure 1A and 1B). In the image processing step, acquired images are processed to correct for image distortion as well as removal of features that are not of interest, such as the skull and the superficial soft tissue. The remaining images are then projected onto a standardized template in preparation for comparative analysis. Image segmentation refers to delineation of the distinct regions of this projected image into regions of interest, such as regions of CE. This segmentation step can be done by expert reviewers or by semi- or fully automated algorithms.[21,22] Feature extraction refers to the extraction of image characteristics and converting them into quantitative measures. These image characteristics may be obvious to the human eye or difficult to identify, even for expert reviewers. Mathematical models are then constructed to determine association between image features and outcomes of interest, such as survival. These models include linear or logistic regressions as well as more complex models developed in machine learning[23] and deep learning models.[24] Reproducibility of parameter associations is then tested through internal cross-validation followed by validation through an independent external cohort.

TABLE. List of Abbreviations

2-HG	2-Hydroxyglutarate
a-KG	Alpha keto-glutarate
ADC	Apparent diffusion coefficient
ASL	Arterial spin labeling
CE	Contrast enhancement
DCE	Dynamic contrast enhanced
DKI	Diffusion kurtosis imaging
DSC	Dynamic susceptibility contrast-enhanced
DWI	Diffusion weighted imaging
GLSZM	Gray level size zone matrix
IDH	Isocitrate dehydrogenase
IPVL	Iterative probabilistic voxel labeling
LVd	Lateral ventricle displacement
MET	L-Methyl-11C-methionine
MGMT	O6-methylguanine-DNA methyltransferase
MGMTp	MGMT promoter
PET	Positron emission tomography
PRC	Precision-recall curve
rCBV	Relative cerebral blood volume
SVM	Support vector machine
SVZd	Subventricular zone distance
TCGA	The Cancer Genome Atlas
TCIA	The Cancer Imaging Atlas
VEGF	Vascular endothelial growth factor

PREDICTION OF IDH MUTATION

Recurrent mutations in the IDH genes define a subclass of glioblastomas that exhibit distinct clinical course and therapeutic response.[25,26] In their native form, IDH proteins catalyze the conversion of isocitrate into alpha-ketoglutarate.[27] Oncogenic mutations inactivate this enzymatic activity and confer a neomorphic function of producing 2 hydroxyglutarate (2HG).[27] High levels of 2HG, in turn, induce global methylation of the genome resulting in altered gene expression and phenotype.[28] There is great interest in imaging biomarkers that discriminate IDH-mutated glioblastomas from their wild-type counterparts,[29] since the benefit of medical and surgical intervention differs in patients afflicted with these tumors.[30] While the direct detection of 2HG through MR spectroscopy holds tremendous promise in IDH mutation detection, dedicated protocols and expertise are required for implementation, which may not be available to many centers. Moreover, optimal methods for detection (eg, 3T spectroscopy vs 7T spectroscopy, parameterization of MR sequences, etc) remain an area of active investigation. In this context, we have focused our review here on radiomic analysis of MR features available on routine clinical imaging.

Using MR sequences commonly employed in brain tumor imaging (T1, contrast-enhancing T1, and T2-weighted images), Li et al[18] extracted 1614 imaging features from 225 glioblastoma patients. Among the various features tested, imaging features that reflect peritumoral edema performed best for IDH mutation discrimination using precision-recall curves (PRCs). More specifically, gray level size zone matrix features, which create "zones" based on the number of voxels sharing gray level intensities, represented the largest number of features used to successfully predict IDH status. Using these features, a random forest algorithm was trained to achieve a 96% prediction accuracy (area under the curve: 0.9, F1-score: 0.78), and improved when patient age was incorporated. Other studies reported similar detection performance for IDH-mutated gliomas using these standard imaging sequences.[31-34]

While dynamic susceptibility contrast (DSC)-MRIs are used in select centers for brain tumor imaging, this clinical workflow is not universal across all centers. Sudre et al[35] studied

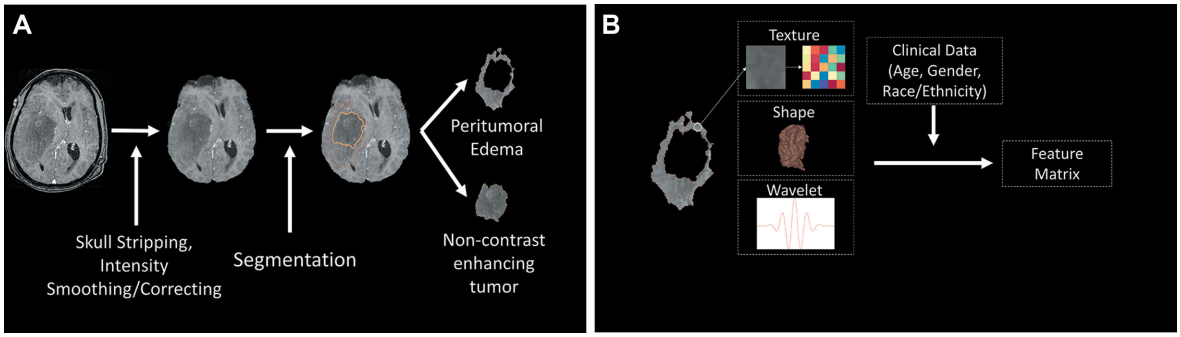

FIGURE 1. *General workflow describing the radiomic image processing steps.* **A**, *Illustration of image processing and image segmentation.* **B**, *Illustration of features extraction and model building.*

333 patients from 6 tertiary centers who underwent DSC-MRI and extracted 29 radiomic features from normalized relative cerebral blood volume (rCBV) maps. The tumor surface-to-volume ratio (a measure of noncompactness) and variance in rCBV were significantly lowered in IDH-mutated tumors. Using these features, a random forest algorithm predicted IDH mutation status with a specificity of 77% and a sensitivity of 65%. Similar results were reported by Kickingereder et al[36] in a study of 73 patients, where the authors noted that IDH-mutated gliomas exhibited lower rCBVs relative to their wild-type counterparts.[36] Using a histogram for rCBV values, each unit increase was associated with a decrease in the likelihood of IDH mutation. The positive and negative predictive values of this method were 89% and 78%, respectively.[36] Other methods of assessing tumor perfusion have also been explored as means of IDH mutation detection and showed comparable performance relative to DSC.[37,38]

Radiomic studies of diffusion-based MRI suggest the utility of apparent diffusion coefficient (ADC) maps in IDH mutation detection. In a study of 142 patients with high-grade gliomas, texture features were extracted from T1 postcontrast, T2, and fluid-attenuated inversion-recovery (FLAIR) MRIs as well as ADC maps.[39] A random forest model that incorporated features derived from these images achieved a diagnostic accuracy of 82.2% across independent cohorts. In their analysis, kurtosis (a measure of the flatness of an image's distribution of the intensity histogram) and skewness (a measure of an image's symmetry of intensity histograms) played a significant role in IDH status determination, but were not shown to be as important as wavelet based features. Similar results have been reported in radiomic studies involving other forms of diffusion MRIs, including diffusion kurtosis imaging (DKI).[40-42] A support vector machine (SVM) trained on the textural features of DKI achieved an accuracy of 81% for IDH mutation detection in gliomas.[40] These results suggest that diffusion imaging alone is insufficient to achieve IDH mutation detection in the clinical setting.

While reasonable detection performances have been reported for IDH mutation,[43] the actual clinical performance will vary depending on the prevalence of the mutation. For grade II and III gliomas, where IDH mutations are more prevalent,[25] the reported performance may be sufficient for consideration of clinical translation. On the other hand, in glioblastomas, the most common form of glioma, the prevalence of IDH mutation is estimated to be less than 10%.[25] As such, concrete progress measured by the imbalance-sensitive PRC will be needed before clinical translation should be considered for this patient population.

In principle, detection performance can be improved by multiparametric modeling that incorporates informative features from across a variety of imaging modalities, including the above-discussed MRI sequences, positron emission tomography (PET),[44-46] and ultrasound.[47] However, the number of imaging modalities that can be adopted during routine work-up for gliomas will be limited by institutional clinical workflow and the availability of select techniques.

PREDICTION OF MGMT PROMOTER METHYLATION

MGMT encodes an evolutionarily conserved DNA repair protein that directly detoxifies cytotoxic DNA damage resulting from the administration of temozolomide,[48] the standard-of-care chemotherapy for glioblastomas.[49] In independent clinical trials, the level of MGMT expression was inversely correlated with clinical survival after temozolomide treatment.[50-53] The expression of MGMT in glioblastomas is regulated both transcriptionally[54] and post-transcriptionally.[55] In terms of transcriptional regulation, methylation of the MGMT promoter (MGMTp) region is associated with suppression of gene expression. As such, MGMTp methylation confers an increased likelihood of therapeutic response to temozolomide.[50] Post-transcriptionally, key miRNAs, including miR-181d[56] and miR-603,[55] downregulate MGMT expression. In independent cohorts of patients afflicted with MGMTp unmethylated glioblastomas,

high levels of miR-181d and miR-603 were associated with decreased MGMT expression and conferred improved clinical survival in glioblastoma patients who underwent temozolomide therapy.[55]

Diagnostic studies predicting MGMT used a variety of MR modalities, including conventional MRI, diffusion weighted imaging, DSC, and MR-PET.[57-60] In terms of T1- and T2-based radiomics, Korfiatis et al[59] carried out a retrospective analysis of 155 patients with known MGMTp methylation status and compared the texture features derived from postcontrast T1 and T2 images. Imaging features that most discriminated MGMTp methylation status captured measures of intensity uniformity and symmetry including cluster prominence and cluster shade. An SVM-based classification predicted MGMTp methylation status with 80% sensitivity and 81% specificity.[59] These results were recapitulated by others.[60,61] For instance, Kanas et al[57] reported that MGMTp unmethylated tumors tend to exhibit more homogenous CE, while MGMTp methylated tumors tend to exhibit ring CE, with central necrosis as well as decreased peritumoral edema. While some studies reported that MGMTp unmethylated glioblastomas tend to carry larger areas of necrosis[62] and be located in the right hemisphere[63] or the frontal lobe,[64] conflicting results were also reported. Independent studies have reported that MGMTp unmethylated glioblastomas are more likely located in proximity to the SVZ.[65,66]

On diffusion imaging, MGMTp methylated glioblastomas showed higher ADC values relative to their unmethylated counterparts.[67] Moreover, the MGMTp methylated glioblastomas were more likely to harbor lowered relative cerebral blood flow in studies involving DSC[68] and arterial spin labeling.[66] Using PET imaging, MGMTp methylated glioblastomas have shown increased FDG uptake while exhibiting comparable MET uptake.[69] The sensitivity and specificity of discrimination using these modalities are largely comparable to those reported for T1- and T2-based MRI.[57,58,60,59,70] To date, multimodality integration has not significantly improved discriminatory capacity.[58] A recent meta-analysis of high-quality studies that aimed to predict MGMTp methylation status using radiomic approaches showed a pooled sensitivity and specificity of 79% and 73%, respectively.[71] As with IDH mutation detection, reported performances lie below the understood threshold of reliable detection needed to guide clinical decision making.

MOLECULAR PHYSIOLOGY OF CONTRAST ENHANCEMENT

Glioblastoma is the most common form of primary brain cancer in adults and remains a major therapeutic challenge in neuro-oncology.[72] Molecular profiling of clinical specimens derived from affected patients reveals significant intertumoral heterogeneity. That is, specimens with similar histopathological appearances nevertheless exhibit distinct molecular profiles.[73]

CE is a feature shared by most glioblastomas.[11] There have been several radiomic studies that investigated whether textural elements of CE reflect aspects of tumor physiology. Classically, CE on glioblastoma imaging is thought to reflect tumor-related alterations in vascular permeability.[74] Subsequent radiomic studies have expanded on this understanding. In a study of 22 patients, Diehn et al[75] reported that an increased number of voxels with CE in glioblastomas were associated with higher mRNA expression of vascular endothelial growth factor (VEGF), a master regulatory protein that governs vascular permeability. In a larger study of 52 patients, Pope et al[76] noted higher VEGF expression in glioblastomas that were completely enhancing relative to those that were incompletely enhancing. Higher mRNA expression of VEGF in glioblastomas rated as highly contrast enhancing was also noted by Jamshidi et al[77] in a study of 23 patients. While other correlations with gene expression were noted, the VEGF finding was the only one shared across the 3 studies.

An association between VEGF expression and CE was confirmed in a fourth study that segmented 148 MRIs available in The Cancer Imaging Atlas (TCIA).[73] This study additionally explored gene expression patterns associated with the various radiomic features of CE, including mean normalized intensity (CE_i; Figure 2A), heterogeneity in CE (measured by the total variance in CE, noted as CE_h; Figure 2B), and the ratio of CE voxel as a function of total tumor volume (CE_r; Figure 2C).[73] Correlative analysis suggests that high CE_r is associated with gene expression patterns suggestive of stressful metabolic conditions, including hypoxia.

HIGHER ORDER RADIOMIC FEATURES

Two higher order radiomic features will be reviewed in this section: SVZd and lateral ventricle displacement (LVd). These features were developed based on insights gained through studies conducted in the basic and clinical neurosciences.

Distance to the Subventricular Zone

During the development of the human brain, neuronal precursor cells migrate radially from the stem cell niche in the subventricular zone (SVZ).[78] Neural precursor cells lose their stem cell property of self-renewal and differentiate into distinct cell types as they migrate, forming layers of cytoarchitectures.[78,79] There is evidence that glioblastomas may arise from cell types that differ in their radial distances from the SVZ and inherit the intrinsic properties of these precursor cells. As such, SVZd may be an imaging marker for the "stemness" of a tumor and for poor clinical survival (Figure 3).

The irregular morphology of most glioblastomas presents a significant challenge in the calculation of SVZd. Steed et al[65] analyzed TCIA glioblastomas to show those in proximity to the SVZ are more likely to harbor mRNA expression profiles that indicate neural stem cell states. Accordingly, patients afflicted with

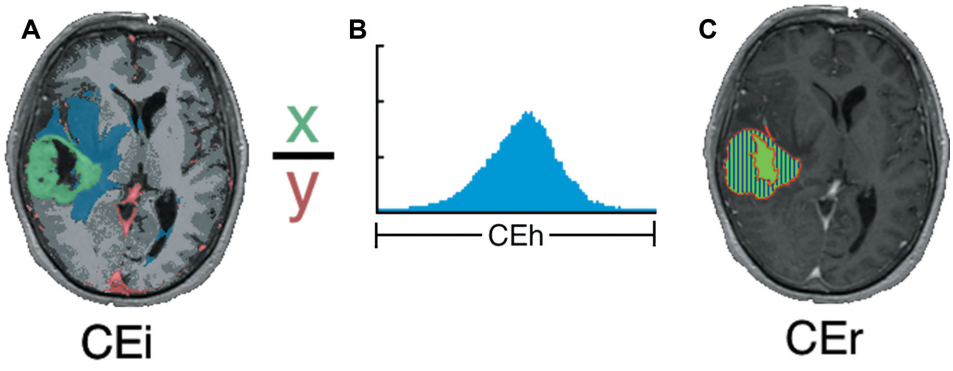

FIGURE 2. **A**, *Using a selected patient from The Cancer Genome Atlas, mean normalized intensity (CE_i) is derived from the ratio of mean voxel intensity in the contrast-enhancing region (green) to the median voxel intensity of blood vessels (red).* **B**, *As a way to capture voxel intensity heterogeneity, CE_h, is derived from the Shannon entropy of the contrast-enhancing region.* **C**, *CE_r is defined as the ratio of the volume of contrast-enhancing tumor (red outline with blue stripes) to the volume of the filled contrast-enhancing region (green). Reprinted from Steed TC, Treiber JM, Brandel MG, et al. Quantification of glioblastoma mass effect by lateral ventricle displacement. Sci Rep. 2018;8:2827. Under the Creative's Commons License (http://creativecommons.org/licenses/by/4.0/).*

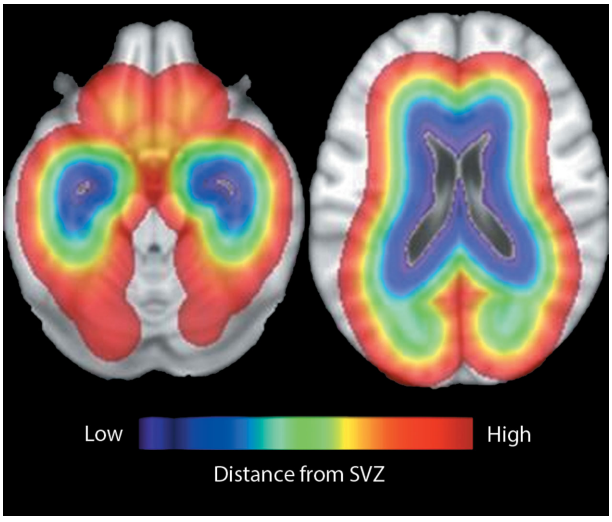

FIGURE 3. *A color-coded atlas brain showing how distances from the subventricular zone (SVZ) within the lateral ventricle can be quantitatively determined. Glioblastoma centroids falling within the blue region represent those arising closer to the ependymal surface, while those falling within the red region represent those arising further away from the ependymal surface. Reprinted from Steed TC, Treiber JM, Brandel MG, et al. Quantification of glioblastoma mass effect by lateral ventricle displacement. Sci Rep. 2018;8:2827. Under the Creative's Commons License (http://creativecommons.org/licenses/by/4.0/).*

SVZ proximal tumors exhibited poor survival relative to those afflicted with SVZ distal tumors.

These findings suggest that SVZd may constitute an imaging biomarker for glioblastomas that are enriched for stem-cell properties. Moreover, therapies targeting these properties[80] may demonstrate higher efficacy against SVZ proximal glioblastomas.

Lateral Ventricular Displacement

The importance of mass effect as a prognostic imaging biomarker is well recognized in clinical neurosurgery.[81] Pertaining to neuro-oncology, mass effect refers to the displacement of the cerebrum secondary to tumor growth; it is a major cause of neurological morbidity and mortality.[82] The extent of mass effect is difficult to determine given interpatient differences in the volume and compliance of the cerebrum.[83] In fact, patients with comparable glioblastoma tumor burden, as gauged by CE volume and FLAIR hyperintensity, often exhibit significant differences in the extent of mass effect.[84]

In clinical practice, mass effect is often noted as "midline shift" or various forms of herniations.[85] However, assessment of these qualitative measures differs between clinicians[86] and is unduly influenced by variability in imaging protocols.[87] To address these shortcomings, LVd was developed as a higher order radiomic measure of mass effect (Figure 4). LVd measures the 3-dimensional vector displacement of the centroid of the lateral ventricle volume in glioblastoma patients relative to the same centroid in a standard Montreal Neurological Institute (MNI) template brain.[88] An analysis of the iterative probabilistic voxel labeling segmented TCIA glioblastoma MRIs showed that the LVd of glioblastoma patients is highly elevated relative to 550 nontumor control subjects.[84] Expectedly, LVd poorly correlated with CE volume and FLAIR hyperintensity, 2 variables frequently used to approximate the glioblastoma tumor burden. While no survival association was observed with the volume of CE or FLAIR hyperintensity, a robust survival association was observed between LVd and clinical survival, after controlling for

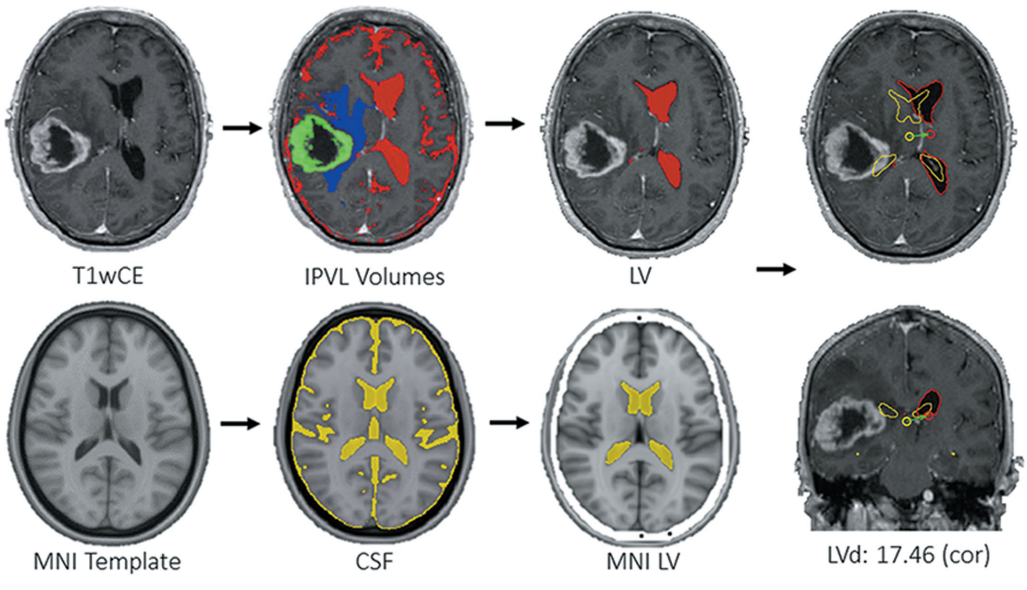

FIGURE 4. *Top row: using an automated segmentation method, T1-weighted contrast-enhancing (T1wCE) scans are segmented into regions of interest (CSF, blood vessels, contrast-enhancing region, flair hyperintensity), including the lateral ventricle (LV). Bottom row: through automated segmentation, an atlas brain (the Montreal Neurological Atlas template; MNI) is used to define a reference CSF volume. Subsequently, each patient's derived LV vector is then compared to this reference atlas LV vector to derive a magnitude of net displacement. Reprinted from Steed TC, Treiber JM, Brandel MG, et al. Quantification of glioblastoma mass effect by lateral ventricle displacement. Sci Rep. 2018;8:2827. Under the Creative's Commons License (http://creativecommons.org/licenses/by/4.0/).*

confounding variables, including age and Karnosfky performance score.

To better understand the biology underlying differential LVd, correlative analyses were performed to compare the mRNA expression of high and low LVd glioblastomas. The analyses indicated that glioblastomas with high LVd exhibited gene signatures associated with cell growth, while glioblastomas with low LVd showed signatures associated with invasion. Notably, LVd and SVZd were independently associated with survival,[84,89] consistent with the idea that the 2 parameters convey distinct underlying physiological states.

DISCUSSION AND CONCLUSION

Here, we provided an overview of current and emerging strategies in radiomics and reviewed their application in neuro-oncology. Given the current state of glioblastoma radiomics, it is not possible to definitively conclude which features are most important for survival prognostication. To the extent that survival prognostication requires synthesis of SVZd and LVd, it is likely that optimal prognostication will require integration of multiple informative imaging features. The prognostic interaction between IDH mutation and MGMT promoter methylation[90] further supports this conclusion. While tools in machine learning are available to delineate the relative importance of each prognostic factors, such analysis has not been carried out using the features described in this review and constitute an important direction of future research.

It is important to note that survival prognostication represents a small segment of the vast potential for radiomics to impact clinical neurosurgery. Other applications include the differentiation of glioblastoma from other pathologies,[91,92] discrimination of glioma grades,[93,94] identification of mutations and amplifications,[95] determining pseudoprogression versus tumoral progression.[96] In this context, radiomics holds tremendous potential in advancing our understanding of the *in vivo* physiology of brain tumors as they exist in the patient and offers opportunities for optimizing clinical care of brain tumor patients.

Funding

This study did not receive any funding or financial support.

Disclosures

The authors have no personal, financial, or institutional interest in any of the drugs, materials, or devices described in this article.

REFERENCES

1. Ginsburg GS, Phillips KA. Precision medicine: from science to value. *Health Aff.* 2018;37(5):694-701.
2. Vives KP, Piepmeier JM. Complications and expected outcome of glioma surgery. *J Neurooncol.* 1999;42(3):289-302.

3. Parker NR, Khong P, Parkinson JF, Howell VM, Wheeler HR. Molecular heterogeneity in glioblastoma: potential clinical implications. *Front Oncol*. 2015;5:55.
4. Dina Randazzo KBP. Psychosocial distress and its effects on the health-related quality of life of primary brain tumor patients. *CNS Oncol*. 2016;5(4):241-249.
5. Randazzo DM, McSherry F, Herndon JE, et al. A cross sectional analysis from a single institution's experience of psychosocial distress and health-related quality of life in the primary brain tumor population. *J Neurooncol*. 2017;134(2):363-369.
6. Muragaki Y, Chernov M, Maruyama T, et al. Low-grade glioma on stereotactic biopsy: how often is the diagnosis accurate? *Minim Invasive Neurosurg*. 2008;51(5):275-279.
7. Jackson RJ, Fuller GN, Abi-Said D, et al. Limitations of stereotactic biopsy in the initial management of gliomas. *Neuro Oncol*. 2001;3(3):193-200.
8. Patel AP, Tirosh I, Trombetta JJ, et al. Single-cell RNA-seq highlights intratumoral heterogeneity in primary glioblastoma. *Science*. 2014;344(6190):1396-1401.
9. Abrams DA, Hanson JA, Brown JM, Hsu FPK, Delashaw JB Jr, Bota DA. Timing of surgery and bevacizumab therapy in neurosurgical patients with recurrent high grade glioma. *J Clin Neurosci*. 2015;22(1):35-39.
10. Gevaert O, Xu J, Hoang CD, et al. Non–small cell lung cancer: identifying prognostic imaging biomarkers by leveraging public gene expression microarray data—methods and preliminary results. *Radiology*. 2012;264(2):387-396.
11. Gutman DA, Cooper LAD, Hwang SN, et al. MR imaging predictors of molecular profile and survival: multi-institutional study of the TCGA glioblastoma data set. *Radiology*. 2013;267(2):560-569.
12. Zinn PO, Singh SK, Kotrotsou A, et al. Distinct radiomic phenotypes define glioblastoma TP53-PTEN-EGFR mutational landscape. *Neurosurgery*. 2017;64(CN_Suppl_1):203-210.
13. Rathore S, Akbari H, Doshi J, et al. Radiomic signature of infiltration in peritumoral edema predicts subsequent recurrence in glioblastoma: implications for personalized radiotherapy planning. *J Med Imaging*. 2018;5(2):021219.
14. Oh J, Cha S, Aiken AH, et al. Quantitative apparent diffusion coefficients and T2 relaxation times in characterizing contrast enhancing brain tumors and regions of peritumoral edema. *J Magn Reson Imaging*. 2005;21(6):701-708.
15. Park JE, Kickingereder P, Kim HS. Radiomics and deep learning from research to clinical workflow: neuro-oncologic imaging. *Korean J Radiol*. 2020;21(10):1126-1137.
16. Bae S, Choi YS, Ahn SS, et al. Radiomic MRI phenotyping of glioblastoma: improving survival prediction. *Radiology*. 2018;289(3):797-806.
17. Ostrom QT, Gittleman H, Truitt G, Boscia A, Kruchko C, Barnholtz-Sloan JS. CBTRUS statistical report: primary brain and other central nervous system tumors diagnosed in the United States in 2011-2015. *Neuro Oncol*. 2018;20(Suppl_4):iv1-iv86.
18. Li Z-C, Bai H, Sun Q, et al. Multiregional radiomics profiling from multiparametric MRI: identifying an imaging predictor of IDH1 mutation status in glioblastoma. *Cancer Med*. 2018;7(12):5999-6009.
19. Eichinger P, Alberts E, Delbridge C, et al. Diffusion tensor image features predict IDH genotype in newly diagnosed WHO grade II/III gliomas. *Sci Rep*. 2017;7(1):13396.
20. Lin Y, Xing Z, She D, et al. IDH mutant and 1p/19q co-deleted oligodendrogliomas: tumor grade stratification using diffusion-, susceptibility-, and perfusion-weighted MRI. *Neuroradiology*. 2017;59(6):555-562.
21. Lai X, Xu X, Li W. Automatic glioblastoma segmentation in multimodal MR images using improved fully convolutional neural networks. *J Med Imaging Hlth Inform*. 2019;9(7):1407-1414.
22. Yushkevich PA, Gao Y, Gerig G. ITK-SNAP: an interactive tool for semi-automatic segmentation of multi-modality biomedical images. *Conf Proc IEEE Eng Med Biol Soc*. 2016;2016:3342-3345.
23. Suter Y, Knecht U, Alão M, et al. Radiomics for glioblastoma survival analysis in pre-operative MRI: exploring feature robustness, class boundaries, and machine learning techniques. *Cancer Imaging*. 2020;20(1):55.
24. Lao J, Chen Y, Li Z-C, et al. A deep learning-based radiomics model for prediction of survival in glioblastoma multiforme. *Sci Rep*. 2017;7(1):10353.
25. Yan H, Parsons DW, Jin G, et al. IDH1 and IDH2 mutations in gliomas. *N Engl J Med*. 2009;360(8):765-773.
26. Cancer Genome Atlas Research Network, Brat DJ, Verhaak RGW, et al. Comprehensive, integrative genomic analysis of diffuse lower-grade gliomas. *N Engl J Med*. 2015;372(26):2481-2498.
27. Reitman ZJ, Yan H. Isocitrate dehydrogenase 1 and 2 mutations in cancer: alterations at a crossroads of cellular metabolism. *J Natl Cancer Inst*. 2010;102(13):932-941.
28. Bledea R, Vasudevaraja V, Patel S, et al. Functional and topographic effects on DNA methylation in IDH1/2 mutant cancers. *Sci Rep*. 2019;9(1):16830.
29. Chaddad A, Kucharczyk MJ, Daniel P, et al. Radiomics in glioblastoma: current status and challenges facing clinical implementation. *Front Oncol*. 2019;9:374.
30. Tateishi K, Wakimoto H, Cahill DP. IDH1 mutation and World Health Organization 2016 diagnostic criteria for adult diffuse gliomas: advances in surgical strategy. *Neurosurgery*. 2017;64(CN_Suppl_1):134-138.
31. Kesler SR, Harrison RA, Petersen ML, et al. Pre-surgical connectome features predict IDH status in diffuse gliomas. *Oncotarget*. 2019;10(60):6484-6493.
32. Han L, Wang S, Miao Y, et al. MRI texture analysis based on 3D tumor measurement reflects the IDH1 mutations in gliomas—a preliminary study. *Eur J Radiol*. 2019;112:169-179.
33. Lewis MA, Ganeshan B, Barnes A, et al. Filtration-histogram based magnetic resonance texture analysis (MRTA) for glioma IDH and 1p19q genotyping. *Eur J Radiol*. 2019;113:116-123.
34. Yu J, Shi Z, Lian Y, et al. Noninvasive IDH1 mutation estimation based on a quantitative radiomics approach for grade II glioma. *Eur Radiol*. 2017;27(8):3509-3522.
35. Sudre C, Panovska-Griffiths J, Sanverdi E, et al. Machine learning assisted DSC-MRI radiomics as a tool for glioma classification by grade and mutation status. *BMC Med Inform Decis Mak*. 2020;20(1):149.
36. Kickingereder P, Sahm F, Radbruch A, et al. IDH mutation status is associated with a distinct hypoxia/angiogenesis transcriptome signature which is non-invasively predictable with rCBV imaging in human glioma. *Sci Rep*. 2015;5(1):1-9.
37. Brendle C, Hempel J-M, Schittenhelm J, et al. Glioma grading and determination of IDH mutation status and ATRX loss by DCE and ASL perfusion. *Clin Neuroradiol*. 2018;28(3):421-428.
38. Lu HT, Xing W, Zhang YW, Qin HP, Wu RH, Ding JL. The value of DCE-MRI in predicting IDH gene mutation of high-grade gliomas. *Zhonghua Yi Xue Za Zhi*. 2019;99(39):3105-3109.
39. Alis D, Bagcilar O, Senli YD, et al. Machine learning-based quantitative texture analysis of conventional MRI combined with ADC maps for assessment of IDH1 mutation in high-grade gliomas. *Jpn J Radiol*. 2020;38(2):135-143.
40. Bisdas S, Shen H, Thust S, et al. Texture analysis- and support vector machine-assisted diffusional kurtosis imaging may allow in vivo gliomas grading and IDH-mutation status prediction: a preliminary study. *Sci Rep*. 2018;8(1):6108..
41. Abdalla G, Mancini L, Eser Sanverdi S, Yousry T, Bisdas S. Diffusion kurtosis imaging identifies the IDH mutation status of gliomas. *Neuro-oncol*. 2018;20(Suppl_5):v351-v351.
42. Zhao J, Wang Y-L, Li X-B, et al. Comparative analysis of the diffusion kurtosis imaging and diffusion tensor imaging in grading gliomas, predicting tumour cell proliferation and IDH-1 gene mutation status. *J Neurooncol*. 2019;141(1):195-203.
43. Zhao J, Huang Y, Song Y, et al. Diagnostic accuracy and potential covariates for machine learning to identify IDH mutations in glioma patients: evidence from a meta-analysis. *Eur Radiol*. 2020;30(8):4664-4674.
44. Li L, Mu W, Wang Y, et al. A non-invasive radiomic method using 18F-FDG PET predicts isocitrate dehydrogenase genotype and prognosis in patients with glioma. *Front Oncol*. 2019;9:1183.
45. Zhao K, Yu P, Xue Z, et al. 11C-Methionine integrated PET/MRI-based texture analysis features may have a potential ability to distinguish oligodendroglioma (IDH-mutant and 1p/19q-codeleted) from varied gliomas. *Acad Radiol*. 2020;27(7):e159-e167.
46. Lohmann P, Lerche C, Bauer EK, et al. Predicting IDH genotype in gliomas using FET PET radiomics. *Sci Rep*. 2018;8(1):13328.
47. Bø HK, Solheim O, Kvistad K-A, et al. Intraoperative 3D ultrasound-guided resection of diffuse low-grade gliomas: radiological and clinical results. *J Neurosurg*. 2019;132(2):518-529.
48. Yu W, Zhang L, Wei Q, Shao A. O6-methylguanine-DNA methyltransferase (MGMT): challenges and new opportunities in glioma chemotherapy. *Front Oncol*. 2020;9:1547.
49. Johnson DR, O'Neill BP. Glioblastoma survival in the United States before and during the temozolomide era. *J Neurooncol*. 2012;107(2):359-364.
50. Hegi ME, Diserens A-C, Gorlia T, et al. MGMT gene silencing and benefit from temozolomide in glioblastoma. *N Engl J Med*. 2005;352(10):997-1003.
51. Sarathy V, Jayappa SB, Lalkota B, et al. Impact of MGMT promoter methylation as a prognostic marker in patients with high grade glioma: a single-center observational study. *J Cancer Therapy*. 2019;10(10):806-814.

52. Preusser M, Hassler M, Elandt K, et al. Analysis of MGMT promoter methylation status in high grade glioma patients with long term and conventional survival times: a retrospective study. *J Clin Oncol*. 2007;25(18_Suppl):2084-2084.
53. Hegi ME, Diserens A-C, Godard S, et al. Clinical trial substantiates the predictive value of O-6-methylguanine-DNA methyltransferase promoter methylation in glioblastoma patients treated with temozolomide. *Clin Cancer Res*. 2004;10(6):1871-1874.
54. Chen X, Zhang M, Gan H, et al. A novel enhancer regulates MGMT expression and promotes temozolomide resistance in glioblastoma. *Nat Commun*. 2018;9(1):2949.
55. Kushwaha D, Ramakrishnan V, Ng K, et al. A genome-wide miRNA screen revealed miR-603 as a MGMT-regulating miRNA in glioblastomas. *Oncotarget*. 2014;5(12):4026-4039.
56. Zhang W, Zhang J, Hoadley K, et al. miR-181d: a predictive glioblastoma biomarker that downregulates MGMT expression. *Neuro Oncol*. 2012;14(6):712-719.
57. Kanas VG, Zacharaki EI, Thomas GA, Zinn PO, Megalooikonomou V, Colen RR. Learning MRI-based classification models for MGMT methylation status prediction in glioblastoma. *Comput Methods Programs Biomed*. 2017;140:249-257.
58. Kickingereder P, Bonekamp D, Nowosielski M, et al. Radiogenomics of glioblastoma: machine learning-based classification of molecular characteristics by using multiparametric and multiregional MR imaging features. *Radiology*. 2016;281(3):907-918.
59. Korfiatis P, Kline TL, Coufalova L, et al. MRI texture features as biomarkers to predict MGMT methylation status in glioblastomas. *Med Phys*. 2016;43(6):2835-2844.
60. Xi Y-B, Guo F, Xu Z-L, et al. Radiomics signature: a potential biomarker for the prediction of MGMT promoter methylation in glioblastoma. *J Magn Reson Imaging*. 2018;47(5):1380-1387.
61. Li Z-C, Bai H, Sun Q, et al. Multiregional radiomics features from multiparametric MRI for prediction of MGMT methylation status in glioblastoma multiforme: a multicentre study. *Eur Radiol*. 2018;28(9):3640-3650.
62. Iliadis G, Kotoula V, Chatzisotiriou A, et al. Volumetric and MGMT parameters in glioblastoma patients: survival analysis. *BMC Cancer*. 2012;12(1):3.
63. Ellingson BM, Cloughesy TF, Pope WB, et al. Anatomic localization of O6-methylguanine DNA methyltransferase (MGMT) promoter methylated and unmethylated tumors: a radiographic study in 358 de novo human glioblastomas. *Neuroimage*. 2012;59(2):908-916.
64. Paldor I, Pearce FC, Drummond KJ, Kaye AH. Frontal glioblastoma multiforme may be biologically distinct from non-frontal and multilobar tumors. *J Clin Neurosci*. 2016;34:128-132.
65. Steed TC, Treiber JM, Taha B, et al. Glioblastomas located in proximity to the subventricular zone (SVZ) exhibited enrichment of gene expression profiles associated with the cancer stem cell state. *J Neurooncol*. 2020;148(3):455-462.
66. Han Y, Yan L-F, Wang X-B, et al. Structural and advanced imaging in predicting MGMT promoter methylation of primary glioblastoma: a region of interest based analysis. *BMC Cancer*. 2018;18(1):1-10.
67. Moon W-J, Choi JW, Roh HG, Lim SD, Koh Y-C. Imaging parameters of high grade gliomas in relation to the MGMT promoter methylation status: the CT, diffusion tensor imaging, and perfusion MR imaging. *Neuroradiology*. 2012;54(6):555-563.
68. Ryoo I, Choi SH, Kim J-H, et al. Cerebral blood volume calculated by dynamic susceptibility contrast-enhanced perfusion MR imaging: preliminary correlation study with glioblastoma genetic profiles. *PLoS One*. 2013;8(8):e71704.
69. Ning J, Yu P, Lin M, et al. Texture analysis of 11C-methinine PET images may facilitate to evaluate the MGMT methylation status in gliomas: based on integrated PET/MR imaging. *J Nucl Med*. 2019;60(Suppl 1):396.
70. Levner I, Drabycz S, Roldan G, De Robles P, Cairncross JG, Mitchell R. Predicting MGMT methylation status of glioblastomas from MRI texture. *Med Image Comput Comput Assist Interv*. 2009;12(Pt 2):522-530.
71. Suh CH, Kim HS, Jung SC, Choi CG, Kim SJ. Clinically relevant imaging features for MGMT promoter methylation in multiple glioblastoma studies: a systematic review and meta-analysis. *AJNR Am J Neuroradiol*. 2018;39(8):1439-1445.
72. Bahadur S, Sahu AK, Baghel P, Saha S. Current promising treatment strategy for glioblastoma multiform: a review. *Oncol Rev*. 2019;13(2):417.
73. Treiber JM, Steed TC, Brandel MG, et al. Molecular physiology of contrast enhancement in glioblastomas: an analysis of The Cancer Imaging Archive (TCIA). *J Clin Neurosci*. 2018;55:86-92.
74. Law M, Yang S, Babb JS, et al. Comparison of cerebral blood volume and vascular permeability from dynamic susceptibility contrast-enhanced perfusion MR imaging with glioma grade. *AJNR Am J Neuroradiol*. 2004;25(5):746-755.
75. Diehn M, Nardini C, Wang DS, et al. Identification of noninvasive imaging surrogates for brain tumor gene-expression modules. *Proc Natl Acad Sci USA*. 2008;105(13):5213-5218.
76. Pope WB, Young JR, Ellingson BM. Advances in MRI assessment of gliomas and response to anti-VEGF therapy. *Curr Neurol Neurosci Rep*. 2011;11(3):336-344.
77. Jamshidi N, Diehn M, Bredel M, Kuo MD. Illuminating radiogenomic characteristics of glioblastoma multiforme through integration of MR imaging, messenger RNA expression, and DNA copy number variation. *Radiology*. 2014;270(1):1-2.
78. Ming G-L, Song H. Adult neurogenesis in the mammalian brain: significant answers and significant questions. *Neuron*. 2011;70(4):687-702.
79. Tan X, Shi S-H. Neocortical neurogenesis and neuronal migration. *Wiley Interdiscip Rev Dev Biol*. 2013;2(4):443-459.
80. Khalifa J, Tensaouti F, Lusque A, et al. Subventricular zones: new key targets for glioblastoma treatment. *Radiat Oncol*. 2017;12(1):1-11.
81. Dallabona M, Sarubbo S, Merler S, et al. Impact of mass effect, tumor location, age, and surgery on the cognitive outcome of patients with high-grade gliomas: a longitudinal study. *Neurooncol Pract*. 2017;4(4):229-240.
82. Pouratian N, Asthagiri A, Jagannathan J, Shaffrey ME, Schiff D. Surgery Insight: the role of surgery in the management of low-grade gliomas. *Nat Rev Neurol*. 2007;3(11):628-639.
83. Tameem A, Krovvidi H. Cerebral physiology. *Contin Educ Anaesth Crit Care Pain*. 2013;13(4):113-118.
84. Steed TC, Treiber JM, Brandel MG, et al. Quantification of glioblastoma mass effect by lateral ventricle displacement. *Sci Rep*. 2018;8(1):2827.
85. Kress J, Schmidt G, Hall J. *Principles of Critical Care*, 4th edn. New York: McGraw-Hill Education /Medical; 2015.
86. Chun KA, Manley GT, Stiver SI, et al. Interobserver variability in the assessment of CT imaging features of traumatic brain injury. *J Neurotrauma*. 2010;27(2):325-330.
87. Um H, Tixier F, Bermudez D, Deasy JO, Young RJ, Veeraraghavan H. Impact of image preprocessing on the scanner dependence of multi-parametric MRI radiomic features and covariate shift in multi-institutional glioblastoma datasets. *Phys Med Biol*. 2019;64(16):165011.
88. Evans AC, Janke AL, Collins DL, Baillet S. Brain templates and atlases. *Neuroimage*. 2012;62(2):911-922.
89. Steed TC, Treiber JM, Taha BR, et al. Glioblastomas located in proximity to the subventricular zone (SVZ) exhibited enrichment of gene expression profiles associated with the cancer stem cell state. *J Neurooncol*. 2020;148(3):455-462.
90. Molenaar RJ, Verbaan D, Lamba S, et al. The combination of IDH1 mutations and MGMT methylation status predicts survival in glioblastoma better than either IDH1 or MGMT alone. *Neuro Oncol*. 2014;16(9):1263-1273.
91. Kim Y, Cho H-H, Kim ST, Park H, Nam D, Kong D-S. Radiomics features to distinguish glioblastoma from primary central nervous system lymphoma on multi-parametric MRI. *Neuroradiology*. 2018;60(12):1297-1305.
92. Chen C, Ou X, Wang J, Guo W, Ma X. Radiomics-based machine learning in differentiation between glioblastoma and metastatic brain tumors. *Front Oncol*. 2019;9:806.
93. Tian Q, Yan L-F, Zhang X, et al. Radiomics strategy for glioma grading using texture features from multiparametric MRI. *J Magn Reson Imaging*. 2018;48(6):1518-1528.
94. Cho H-H, Lee S-H, Kim J, Park H. Classification of the glioma grading using radiomics analysis. *PeerJ*. 2018;6:e5982.
95. Dong F, Zeng Q, Jiang B, et al. Predicting epidermal growth factor receptor gene amplification status in glioblastoma multiforme by quantitative enhancement and necrosis features deriving from conventional magnetic resonance imaging. *Medicine*. 2018;97(21):e10833.
96. Abrol S, Kotrotsou A, Hassan A, et al. Radiomic analysis of pseudo-progression compared to true progression in glioblastoma patients: a large-scale multi-institutional study. *J Clin Oncol*. 2017;35(15_Suppl):2015-2015.